CHEMISTRY
A EUROPEAN JOURNAL

DOI: 10.1002/chem.200901870

Highly Sensitive Indicator-Free Impedance Sensing of DNA Hybridization Based on Poly(*m*-aminobenzenesulfonic acid)/TiO_2 Nanosheet Membranes with Pulse Potentiostatic Method Preparation

Yu-Wei Hu, Tao Yang, Xin-Xing Wang, and Kui Jiao*[a]

Abstract: A direct electrochemical detection procedure for DNA hybridization by using the electrochemical signal changes of conductive poly(*m*-aminobenzenesulfonic) acid (PABSA)/TiO_2 nanosheet membranes, which were electropolymerized by using the pulse potentiostatic method, is reported. Due to the unique properties of TiO_2 nanoparticles, *m*-aminobenzenesulfonic acid monomers tend to be adsorbed around the particles, and the electropolymerization efficiency is greatly improved. The combination of TiO_2 nanoparticles and PABSA resulted in a nanocomposite membrane with unique and novel nanosheet morphology that provides more activation sites and enhances the surface electron-transfer rate. These characteristics were propitious for the magnification of PABSA electrochemical signals and the direct detection of DNA hybridization. Owing to the presence of abundant sulfonic acid groups, PABSA could overcome the drawbacks of polyaniline and be used to detect bioanalytes at physiological pH. DNA probes could be covalently attached to the sulfonic groups through the amines of DNA sequences by using an acyl chloride cross-linking reaction. After immobilization of probe DNA, the electrochemical impedance value increased significantly compared to that of PABSA/TiO_2 nanosheet membranes, and then decreased dramatically after the hybridization reaction of the probe DNA with the complementary DNA sequence compared to that of the probe-immobilized electrode. Electrochemical impedance spectroscopy was adopted for indicator-free DNA biosensing, which had an eminent ability for the recognition between double-base mismatched sequences or non-complementary DNA sequences and complementary DNA sequences. A gene fragment, which is related to one of the screening genes for the transgenically modified plants, the cauliflower mosaic virus 35S gene was satisfactorily detected. This is the first report for the indicator-free impedance DNA hybridization detection by using PABSA/TiO_2 membranes under neutral conditions.

Keywords: DNA · indicator-free impedance · membranes · nanostructures · pulse potentiostatic method

Introduction

Nucleic acid detection is highly significant in diagnostics, genomics, and clinical medicine. Most strategies for nucleic acid detection require a DNA hybridization event, which could be monitored by either labeled[1] or label-free[2,3] methods. Label assays identify the target analyte, which has been previously modified with a linked label such as enzymes, heterocyclic dyes, ferrocene derivatives, or organometallic complexes.[4] Because the incorporation of a labeling step into a nucleic acid assay is complex, cumbersome, expensive, and time-consuming,[5] the direct and label-free electrochemical detection of DNA hybridization has received considerable interest.[2,3] These techniques rely on either the electrochemical oxidation of bases,[6] or the electrical property changes of an interface along with the structure changes from flexible ssDNA (ss = single strand) to the rigid dsDNA (ds = double strand). The former needs a highly electrocatalytic platform[7] to achieve satisfactory detection sensitivity. The latter is easier for the fabrication of a sensing film, that is, the film for the electrochemical impedance spectroscopy (EIS) detection.[8–11] Compared with voltammetric methods, EIS is a noninvasive method and can be conducted even on insulating substrates for the characteriza-

[a] Y.-W. Hu, Prof. T. Yang, X.-X. Wang, Prof. K. Jiao
Key Laboratory of Eco-chemical Engineering of Ministry of Education
College of Chemistry & Molecular Engineering
Qingdao University of Science & Technology
Qingdao 266042 (China)
Fax: (+86) 532-84023927
E-mail: kjiao@qust.edu.cn

Supporting information for this article is available on the WWW under http://dx.doi.org/10.1002/chem.200901870.

tion of DNA-functionalized electrodes. The immobilization of DNA probes and the hybridization event can induce not only changes in the intrinsic properties of the substrate but also changes in the interfacial properties, such as the capacitance and interfacial electron-transfer resistance. Therefore, by monitoring the changes in electronic or interfacial properties accompanying the DNA immobilization and duplex formation events, the direct and label-free DNA biosensing can be accomplished. A simple, stable and effective conductive route should be overwhelmingly considered for EIS DNA detection.

To construct a sensitive DNA-biosensing platform, various nanomaterials such as gold nanoparticles,[12] carbon nanotubes,[13] and polymers[14,15] have been widely used as a medium of signal amplification and as a probe-immobilization membrane. Compared with gold nanoparticles or carbon-nanotube-based DNA biosensors, the conducting polymer-based DNA biosensor has some advantages, such as low-temperature synthesis and tunable conductivity and no need for purification, end-opening, or catalytic deposition processing.[16] Among polymers, polyaniline (PANI) has a unique position and can be functionalized due to its easy synthesis, good environmental stability, and unique redox tenability. These characteristics make it an attractive material for DNA-biosensing applications. However, the major drawbacks of PANI are its poor solubility in aqueous solution and the loss of its electrochemical activity in solutions of pH greater than 4.[17] These greatly restrict its application in bioelectrochemistry, in which polymers should normally be water-soluble or at least have entire compatibility with the aqueous phase in a neutral pH environment. To overcome these drawbacks, many efforts have been made to introduce functional side-groups (such as COOH, SO_3H, BO_2H_2) into the PANI chains, which form the so-called "self-doped" PANI.[18] The self-doped form of PANI has several advantages including better solubility as well as redox activity and electroconductivity over a wider pH range. One of the "self-doped" PANIs, poly(aminobenzenesulfonic acid) (PABSA), possesses good electrochemical activity and chemical stability,[19,20] and with sulfonic acid groups, PABSA has good solubility and electrocatalytic activities in aqueous solutions with a broad pH range of 1–12 and in most common organic solvents. PABSA has been widely used in the detection of H_2O_2,[20] cytochrome *c*,[21] dopamine and ascorbic acid,[22] NADH, and NAD^+.[23]

Nanosized TiO_2 is technologically important in many applications due to its high surface area per unit volume and good biocompatibility; this greatly increases its activity as a catalyst and sensitivity as a sensor for H_2O_2,[24] DNA,[25] solar cells,[26] HRP,[27] and bioimaging.[28] It should be noted that the presence of nanosized TiO_2 has an obvious influence on the formation of polymers. Zhang reported that the morphology, size, conductivity, and hydrophobicity of the PANI-β-NSA/TiO_2 composite nanotubes (β-NSA:β-naphthalenesulfonic acid) were affected by the TiO_2 nanoparticles.[29]

In the present work, the pulse potentiostatic method (PPM) was used to fabricate nanocomposite sheets in which a PABSA thin layer was formed on a TiO_2 substrate. The formed nanosheets were applied to the indicator-free DNA hybridization detection in a neutral pH environment with EIS. The PABSA/TiO_2 nanosheets combined the high surface area of TiO_2 and the high density of sulfonic acid groups of PABSA together, and could expediently bind the free amines of DNA sequences to sulfonic acid groups of PABSA by using the acyl chloride cross-linking reaction (Figure 1).[30] Specific hybridization of the probe with its

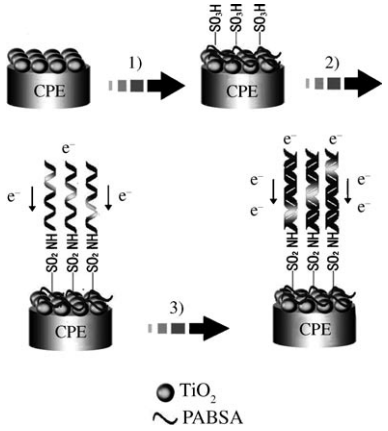

Figure 1. Schematic representation of the immobilization and hybridization of DNA on the PABSA/TiO_2 nanosheets. 1) Electropolymerization; 2) PCl_5 then NH_2–DNA; 3) Hybridization of target DNA.

complementary target DNA sequence induced a significant "signal-on" change in impedance spectroscopy according to frequency variation,[6] which was attributed to the conformational and concomitant conductivity changes of the DNA/PABSA/TiO_2 composite. Electrochemical activities and morphologies of the PABSA/TiO_2 nanosheet-modified carbon paste electrode (CPE) were characterized with cyclic voltammetery (CV) and scanning electron microscopy (SEM), respectively. The influence of electrochemical polymerization factors, such as the substrate, pulse potential, and pulse time on morphology and electrochemical activity of the nanosheets had been studied in detail. CV and EIS were used to investigate the mechanism of the indicator-free electrochemical detection of DNA hybridization. To the best of our knowledge, there are no reports of indicator-free electrochemical sensing of DNA hybridization based on a highly conductive PABSA pathway.

Results and Discussion

Morphology characterization: Electropolymerization is a widely used method to prepare immobilization matrices for DNA hybridization detection, which has the following obvious merits. The thickness, penetrability, and charge-transport characteristics of polymers can be easily controlled by ad-

justing the electrochemical parameters, and the formed polymers have good stability, reproducibility, ample activation sites, homogeneity, and strong adherence to the electrode surface.[21] In this article, polymer-modified electrodes were fabricated by electropolymerization of ABSA. The morphologies of the prepared membrane without and with TiO_2 nanoparticles are shown in Figure 2. Compared with image A (absence of TiO_2), the PABSA on the TiO_2 substrate formed nanosheets that possessed large surface area and lots of gaps among the thin cross-linking sheets (image B). This could also be proved from the side view (image C). This might be due to the presence of TiO_2 nanoparticles with large surface area in the process of electropolymerization of ABSA. When the nanoparticle-modified electrode was immersed into the ABSA solution, ABSA monomers (containing SO_3H function groups) could be adsorbed on the surface of the positively charged TiO_2 nanoparticles (isoelectric point ~5.7)[31] through electrostatic attraction; this results in a considerably higher local concentration of ABSA around TiO_2 nanoparticles. With the application of pulse potentials, ABSA around the TiO_2 was first oxidized to free radicals, and then the polymerization reaction was initiated.[23] Therefore, the polymerization efficiency was greatly improved. In addition, the moderate amount of TiO_2 nanoparticles dispersed in the polymer chain structure gave a more regular structure,[29] which is beneficial for electron transfer along and among polymer chains. Hence, the formed layer possessed excellent electroconductivity. TiO_2 nanoparticles on the polymer chains structure finally resulted in a different, more open, and ramified morphology of the PABSA layer. The resulting PABSA layer had a large surface area and could provide more activation sites and enhance the DNA immobilization amount and steric orientation; this would promote the film efficiency for sensitive DNA detection.

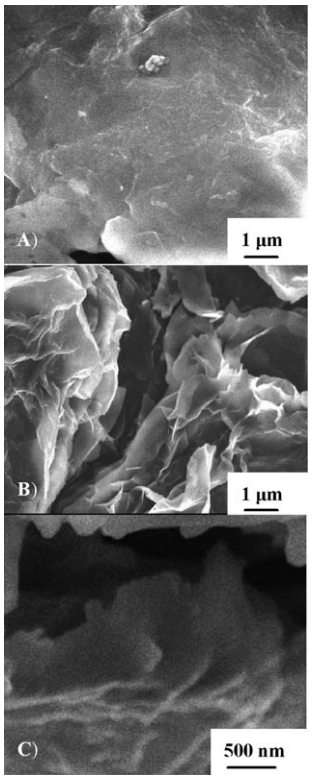

Figure 2. SEM images of the PABSA/CPE (A), PABSA/TiO_2/CPE (top view, B × 5000; side view, C × 10000).

Electrochemical characterization: Compared with traditional electrochemical methods[32] such as the potentiostatic method and the CV method, composites prepared by PPM have larger specific area, higher conductivity, and better reaction ability for the fabrication of electrochemical sensors.[33] Here, the electrochemical properties of PABSA/TiO_2 composites prepared by the CV method and PPM were compared by using $[Fe(CN)_6]^{3-/4-}$ as a classic redox indicator. The peak current obtained from a PABSA/TiO_2 composite prepared by PPM was almost three times as large as that prepared by the CV method. This shows that the PABSA/TiO_2 composite prepared by PPM possesses excellent electroconductivity, which is beneficial for the electron transfer.

CVs of $[Fe(CN)_6]^{3-/4-}$ recorded at the PABSA/TiO_2/CPE and stepwise-modified electrodes prepared by PPM are shown in Figure 3A. Curve a is the CV curve at the bare CPE, which has no well-defined redox peaks. This might be ascribed to the poor electroconductivity of the bare CPE. After bare CPE was modified with TiO_2 nanoparticles, the redox peaks of $[Fe(CN)_6]^{3-/4-}$ became even less visible, as shown in curve b. A couple of well-defined redox peaks

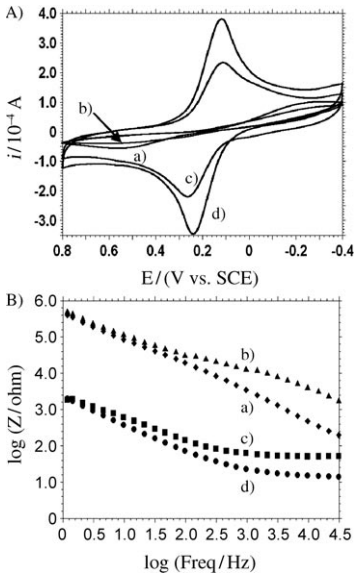

Figure 3. A) CVs of 2.0 mM $[Fe(CN)_6]^{3-/4-}$ (1:1) containing 0.1 M KCl recorded at bare CPE (a), TiO_2/CPE (b), PABSA/CPE (c), and PABSA/TiO_2/CPE (d). Scan rate: 100 mV s^{-1}. B) Bode plots of the electrodes corresponding to (A) recorded in 0.30 M PBS (pH 7.0) under open-circuit conditions. The AC voltage amplitude was 5 mV.

could be observed at the PABSA/CPE (curve c) with a peak potential separation (ΔE_p) of 153 mV. An enhanced couple of redox peaks appeared at the PABSA/TiO_2/CPE (curve d) with a lowered ΔE_p of 122 mV. These results indicate that the PABSA/TiO_2 nanosheets had a much larger effective surface area and good electrical conductivity, which could facilitate the electron transfer of $[Fe(CN)_6]^{3-/4-}$.

The EIS has been employed to investigate the surface properties of the modified electrode and the electron-transfer processes occurring at the electrode–solution interfaces. The Bode plots of modified electrodes were recorded in PBS (pH 7.0) and shown in Figure 3B. An obvious difference in the interface electron-transfer resistances of the above four electrodes could be observed especially in the high-frequency regions. After modification with TiO_2 nanoparticles, the impedance of TiO_2/CPE became larger (curve b) compared to that of bare CPE (curve a). Decreased impedance was obtained at PABSA/CPE (curve c). However, the lowest impedance was observed at PABSA/TiO_2/CPE (curve d), illustrating the lowest electron-transfer resistances. This result is in agreement with that of the CV studies.

Optimization of the fabrication of PABSA/TiO_2 nanosheets

Effect of TiO_2 nanoparticles on the formation of the composite membranes: Two kinds of composite membrane were respectively prepared by using two kinds of TiO_2 nanoparticle addition methods. One was copolymerization of ABSA monomer and TiO_2 nanoparticles, denoted as PABSA-TiO_2. The other was that a certain amount of TiO_2 colloid was firstly dripped on the surface of CPE and then the polymerization was conducted in the ABSA monomer solution, denoted as PABSA/TiO_2. The differential pulse voltammetry (DPV) results of $[Fe(CN)_6]^{3-/4-}$ at the two different types of composite membrane-modified electrodes showed that the current recorded at PABSA/TiO_2/CPE was almost twice as large as that at PABSA-TiO_2/CPE. Thus, the existent form of TiO_2 nanoparticles in electropolymerization had an obvious influence on the electrochemical behavior of the formed nanocomposite membrane. The dripped TiO_2 colloid could form a uniform and compact membrane on the CPE and act as seeds, which could provide more growth sites for the formation of PABSA.

According to the results of the CV, EIS, and DPV measurements mentioned above, the amount of TiO_2 colloid might have a pronounced effect on the performance of the nanosheet-modified electrode. EIS was adopted to optimize the effect of the amount of TiO_2 nanoparticles on the formation of the nanosheets. With increasing TiO_2 amounts, the resistance value of the PABSA/TiO_2 nanosheets was reduced, and the minimum was obtained at 25 μL of 0.01 M TiO_2. If more TiO_2 seeds were used, more PABSA/TiO_2 nanosheets were formed, and fast electron transfer could take place between the PABSA/TiO_2 nanosheets and the electrode surface. However, when the amount of TiO_2 was higher than 25 μL of 0.01 M TiO_2, the resistance value increased. This might be due to the coverage of the electrode surface by an overly dense membrane of TiO_2 nanoparticles, which might prevent the effective adsorption and electropolymerization of ABSA, resulting in the depressed conductivity of the formed nanocomposite. Therefore, 25 μL of 0.01 M TiO_2 was selected for the electrode modification in our experiments.

Selection of pulse potentials: The schematic representation of PPM is shown in Figure S1 (Supporting Information). Five important electropolymerization parameters (upper limit potential E_a, lower limit potential E_c, anodic pulse duration t_a, cathodic pulse duration t_c and total pulse time t_{exp}) for PPM have a pronounced effect on the electroactivities and morphologies of PABSA/TiO_2 nanosheets.[34]

In the electropolymerization process, E_a and E_c were alternated. With the application of E_a, ABSA monomers were polymerized. The polymerization current increased and reached a steady level while the layer reached a thickness that corresponded to nanosheets morphology formation. With the proceeding of polymerization, monomers at the interface of TiO_2-modified electrode/solution were consumed. When the potential suddenly was changed from E_a to E_c, the current descended drastically, polymerization of ABSA ceased even though the monomers were well-supplied, and the formed PABSA changed from the oxidation state to the reduction state.[35] When the voltage was again increased to E_a, the current would reach a steady level, and the oxidation started again. Accordingly, the values of E_a and E_c influenced the morphology and electroconductivity of the PABSA/TiO_2 composite membranes.

If the value of E_a is too big, then ABSA is over-oxidized, and if it is too small, then ABSA is hardly polymerized.[35] The relationship between the values of E_a and the electroconductivity of PABSA/TiO_2/CPE by using $[Fe(CN)_6]^{3-/4-}$ as an indicator was analyzed (Supporting Information, Figure S2). The small value of E_a could not induce the polymerization reaction. When the upper-limit potential was above 1.5 V, the ABSA polymerization reaction was accelerated with the positively shift of the upper limit potential. The maximum peak currents appeared at E_a of 2.2 V. At potentials above 2.2 V, ABSA might be over-oxidized, and the electroconductivity would descend.

The CVs of $[Fe(CN)_6]^{3-/4-}$ recorded at PABSA/TiO_2/CPEs prepared with E_c of different values ranged from −0.8 to −0.3 V were also investigated (Supporting Information, Figure S3). On the basis of the aforementioned discussion, the growth process of PABSA was composed of not only the polymerization of ABSA but also the redox process of the PABSA. The more negative the E_c, the more PABSA changes from oxidization state to reduction state, resulting in the low polymerization efficiency and electron-transfer rate. However, when the E_c was more positive than −0.5 V, little of the PABSA changes from oxidation state to reduction state, and this results in worse reversibility and little current. Therefore, −0.5 V was chosen as the lower limit potential.

Selection of pulse time: The electrochemical behavior of the PABSA/TiO_2 nanosheets was greatly influenced by the polymerization time. According to the following equation,[35] the total oxidation time (t_{ox}) depends on the ratio of t_a/t_c.

$$t_{ox} = t_{\exp}\frac{t_a}{t_a + t_c}$$

In one pulse period (1 s in our experiments), the ratio of t_a to t_c was changed. The relationship between t_a/t_c and the peak current of $[Fe(CN)_6]^{3-/4-}$ at the nanosheet-modified electrode was investigated. The data showed that the peak current increased with the increase of t_a/t_c until $t_a/t_c = 7/3$, and then decreased with further increasing t_a/t_c. If the ratio of t_a/t_c was too low, it was hard for monomers to be polymerized. If the ratio of t_a/t_c was too high (higher than 7/3), the growth rate of PABSA would be too fast, and the consumed monomers would not be compensated in time, which could form the aggregated and over-oxidation state of PABSA. Both had an obvious influence on the electrochemical properties of PABSA, such as poor electroconductivity, less activation sites, and lower electron transfer rate.

With a longer t_{exp}, a thicker membrane might be formed, which might repulse impurities owing to the poor penetrability. That would be a beneficial factor for detecting analytes. However, at the same time, a thicker layer would obstruct electron transfer, which would lower the sensitivity to analytes and prolong the response time, whereas too thin a membrane would have fewer activation sites and the detection of analyte would be easily influenced by impurities. At $t_{exp} = 500$ s, the nanosheets with the highest CV peak currents (Supporting Information, Figure S4) and moderate thickness about 80 nm (Figure 4A) were obtained. When $t_{exp} > 500$ s, the nanosheets could be aggregated. At $t_{exp} = 700$ s, the cross-linked sheets became thicker at almost 160 nm and fewer gaps were obtained (Figure 4B). This could result in the slow diffusion of protons and counter ions into and out of PABSA/TiO_2 nanosheets, and a slow electron-transfer rate. 500 s was chosen as the t_{exp} and t_a/t_c was kept at 7:3.

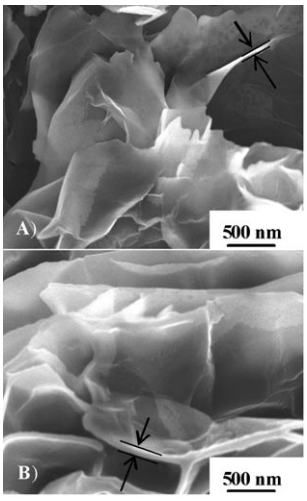

Figure 4. SEM images of the formed PABSA layer with t_{exp} values of A) 500 s and B) 700 s.

CV and indicator-free impedance-based sensing of DNA immobilization and hybridization: After the electropolymerization of the PABSA onto the TiO_2 substrate by PPM, the self-redox properties of the PABSA layer were investigated by the CV and EIS techniques in PBS (pH 7.0). In neutral pH environment, the PABSA layer still retained its electroactivity and bioapplications.[36,37] As shown in Figure 5A,

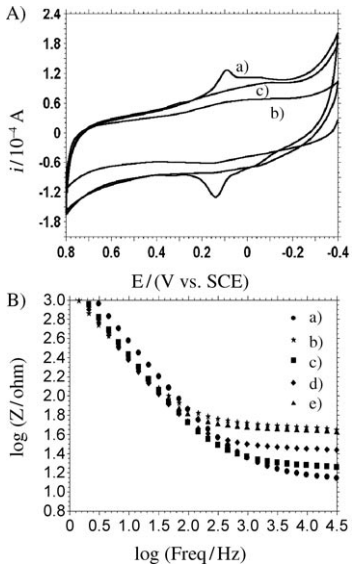

Figure 5. A) CVs of the PABSA/TiO_2 before (a) and after pDNA immobilization (b), hybridization reaction with cDNA (c) recorded in 0.30 M PBS (pH 7.0). Scan rate: 100 mV s^{-1}; B) Bode plots recorded at PABSA/TiO_2/CPE (a), pDNA/PABSA/TiO_2/CPE (b), dsDNA/PABSA/TiO_2/CPE (hybridized with cDNA; c), the probe electrode hybridized with double-base-mismatched DNA (d), the probe electrode hybridized with ncDNA (e) in 0.30 M PBS (pH 7.0) under open-circuit conditions. The AC voltage amplitude was 5 mV.

curve a, well-defined redox peaks between 0.10 V and 0.20 V are observed. This might be due to the self-redox reactions of PABSA that occur at the electrode surface and the redox process going from azobenzene sulfonic acid (anodic peak) to hydrazobenzene sulfonic acid (cathodal peak).[23] When the probe DNA was covalently immobilized on the PABSA layer through the acyl chloride cross-linking reaction, the redox peaks of PABSA almost became invisible, as shown in curve b. This could be attributed to the flexible characteristics and negatively charged phosphate backbones of the probe DNA. After immobilization, probe DNA (pDNA) changed the conformation and blocked the effective electron transfer along the PABSA chains. The obvious decrease in CV signals compared with those of the PABSA layer is strong evidence that pDNA was successfully immobilized on the PABSA layer. After incubation with the complementary DNA (curve c), a significant change of the

shape of CV was observed corresponding to an increased signal in comparison to the signal derived from the CV of the pDNA-captured electrode. The current enhancement upon hybridization might be ascribed to charge distribution, DNA conformation, long-range electron transfer, and rigidity. Hybridization led to changes of conformation. ssDNAs behave as random coils, but dsDNAs (hybridization with the complementary target strand) lead to a more organized surface.[38] The electron transfer or counterion diffusion along the double-helix structure could be freer. At the same time, due to the much higher rigidity of dsDNA compared to ssDNA, the electron transfer rate along the double-helix structure was faster than that along the single-chain structure.[39] Therefore, the self-redox CV signal of polymerization membranes was larger after hybridization of ssDNA with its complementary DNA. The measured current signal could be easily detected by CV without any labeling of probes or target nucleic acids with signaling molecules.

The DNA immobilization and hybridization was also verified by EIS without the use of electroactive indicator. EIS is very sensitive to changes in interfacial impedance upon biorecognition events occurring at the surface–electrolyte interface.[40,41] The EIS measurements were carried out in PBS (pH 7.0) in the frequency range from 1 to 10^5 Hz, and the Bode plots are shown in Figure 5B. Curve a is the Bode plot of PABSA/TiO_2/CPE. When the pDNA was covalently bound onto PABSA/TiO_2 nanosheets, the impedance increased (curve b). The increment of impedance indicated that the pDNA was successfully immobilized on the nanosheets. After hybridization with the complementary DNA (cDNA) sequence under the optimal experimental conditions, the change of the Bode plot was shown in curve c. When the hybridization reaction occurred, an obvious decrease of impedance value was observed.[3,42–44] The EIS result was coincident with the above CV result. Obviously, the PABSA/TiO_2 nanosheets could be used to implement indicator-free direct electrochemical DNA hybridization by EIS detection.

To test whether the indicator-free impedance biosensing of DNA hybridization based on PABSA/TiO_2 nanosheets was sufficiently selective to distinguish target DNA, the pDNA captured electrode was reacted with different DNA sequences (including non-complementary and double-base mismatched sequences), and the Bode plots are shown in Figure 5B. After hybridization with double-base-mismatched sequences, the impedance decreased (curve d), especially in the high-frequency regions.[42,45] However, the decrease in the impedance value was much smaller than that obtained from the hybridization with cDNA (curve c). When the pDNA/PABSA/TiO_2 was hybridized with non-complementary DNA (ncDNA; curve e), the impedance value changed little compared to that of curve b. These results suggested that the indicator-free impedance biosensing of DNA hybridization based on PABSA/TiO_2 nanosheets exhibit good selectivity.

Detection of the sequence-specific CaMV35S gene fragment: The pDNA-captured PABSA/TiO_2 nanosheets were used to detect the cauliflower mosaic virus 35S gene (CaMV35S) target sequences, and the Bode plots were obtained after hybridization with different concentrations of the complementary target sequences (Figure 6A). The difference (namely $\Delta \log Z$) between the $\log Z$ value of the probe-captured electrode and that after hybridization with cDNA was adopted as the measurement signal. The $\Delta \log Z$ value was linear with the logarithm of the CaMV35S gene target sequence concentrations (Figure 6B). The dynamic detection range for the sequence-specific DNA of CaMV35S gene was from 1.0×10^{-11} to 1.0×10^{-6} M with the regression equation $\Delta \log Z = 0.0585 \log C + 0.6893$ and the regression coefficient (γ) 0.9970. The detection limit of this indicator-free impedance detection assay was 1.7×10^{-12} M with 3σ (in which σ was the relative standard deviation of 11 parallel measurements of the blank solution). With the PABSA/TiO_2 nanosheets and an indicator-free direct electrochemical hybridization detection by using EIS, the sensitivity for the CaMV35S gene sequence determination was greatly enhanced.

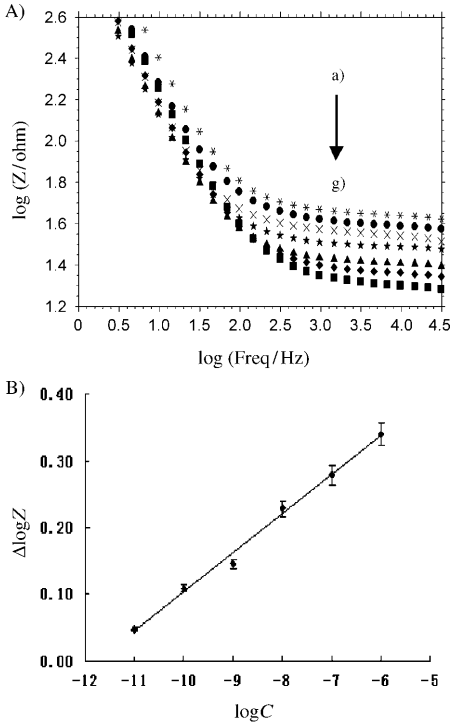

Figure 6. A) Bode plots recorded at the pDNA/PABSA/TiO_2/CPE (a) and after hybridization with its complementary CaMV35S gene sequences of different concentrations: b) 1.0×10^{-11} M, c) 1.0×10^{-10} M, d) 1.0×10^{-9} M, e) 1.0×10^{-8} M, f) 1.0×10^{-7} M, g) 1.0×10^{-6} M. B) The plot of $\Delta \log Z$ vs. the logarithm of CaMV35S gene sequences concentrations. Conditions were the same as in Figure 5B.

The regeneration of a DNA-biosensing assay is achieved by either a thermal or a chemical regeneration procedure. In this work, the regeneration ability of this DNA-biosens-

ing assay was evaluated by denaturing the hybridized dsDNA on the electrode surface. The hybridized dsDNA electrode was denatured by immersing it into 10 mM NaOH for 2 min,[15] followed by rinsing the electrode with ultrapure water, and the regenerated pDNA/PABSA/TiO_2/CPE was used repeatedly. The Bode plots of the regenerated pDNA/PABSA/TiO_2/CPE and the hybridized dsDNA/PABSA/TiO_2/CPE in PBS (pH 7.0) were recorded. The results indicated that the two $\log Z$ values and $\Delta\log Z$ value were, respectively, almost the same values as those obtained in the first experiment. Repetitive experiments showed that the DNA-biosensing assay could be reproduced for three times without losing its sensitivity; this indicates the fine regeneration ability of this DNA-biosensing assay.

The reproducibility of any biosensor is extremely important in DNA detection. In our test, the reproducibility of this indicator-free impedance DNA-biosensing assay was examined by a parallel measurement method. Six parallel immobilizations of 1.0×10^{-6} M probe DNA on the PABSA/TiO_2/CPE were performed and then hybridized, respectively, with 1.0×10^{-6} M target DNA. Bode plots of these electrodes before and after hybridization were recorded and are shown in Figure S5 (Supporting Information). A relative standard deviation (RSD) of 4.91% for the $\Delta\log Z$ value was estimated (Supporting Information, Table S1), which showed the high reproducibility of the DNA-biosensing assay.

The stability of oligonucleotide probes on the modified surface is an important factor, which plays a critical role in obtaining good sensitivity. To investigate the stability of the pDNA/PABSA/TiO_2/CPE, the electrode was incubated in ultrapure water, PBS buffer solution (pH 7.0), Tris–HCl solution (5.0 mM Tris–HCl, 50.0 mM NaCl, pH 7.0), 2×SSC solution (pH 7.0), which consisted of NaCl (0.30 M) and sodium citrate tribasic dihydrate ($C_6H_5Na_3O_7\cdot2H_2O$; 0.030 M), at 25 °C for 6 h, respectively. Then the probe-captured electrode was tested in 0.30 M PBS (pH 7.0) by EIS according to the procedure. The results showed that the incubated electrode had the same behavior as the unincubated electrode and could be applied to the detection of the complementary DNA sequence.

Conclusion

In this paper, a novel platform for indicator-free impedance biosensing of DNA hybridization based on highly conductive PABSA/TiO_2 nanosheets was developed. The PABSA/TiO_2 composite prepared by PPM possessed a nanosheets morphology, which was more open, ramified, possessed a large electroactive area, and increased the efficiency of electron transfer. The PABSA/TiO_2 nanosheets presented good redox activity and electroconductivity even in a neutral environment (PBS solution of pH 7.0). With abundant SO_3H groups, pDNA could be easily and firmly immobilized on the PABSA/TiO_2 nanosheets through covalent binding. Due to the DNA immobilization and hybridization, the DNA/PABSA/TiO_2 hybrid underwent conformational, electroconductive, and interfacial properties changes. These changes were monitored by impedance measurements. The impedance change was adopted as a signal for the indicator-free direct electrochemical DNA hybridization detection. The approach does not require labeling of oligonucleotide probes or targets prior to the assay, and this makes it advantageous in terms of simplicity, noninvasiveness, and low costs.

Experimental Section

Apparatus and materials: All electrochemical experiments were conducted in a standard 3-electrode cell at RT by using a CHI 660B electrochemical workstation (Shanghai CH Instrument Company, Shanghai, China). A Pt wire and a saturated calomel electrode (SCE) were used as the counter and reference electrode, respectively. CPE or the modified CPEs were used as the working electrode. SEM was carried out by using a JSM-5900 machine (JEOL, Tokyo, Japan).

The following parameters were employed for CV and DPV, respectively: CV: scan rate 100 $mV\,s^{-1}$, potential scanning range 0.8–−0.4 V; DPV: pulse amplitude 50 mV, pulse width 60 ms, pulse period 200 ms, potential scanning range 1.0–−0.6 V. Supporting electrolyte was PBS solution (0.30 M; pH 7.0) or $K_3Fe(CN)_6$ (2.0 mM) and $K_4Fe(CN)_6$ (2.0 mM; 1:1) solution containing KCl (0.1 M). The EIS experimental parameters: the AC voltage amplitude was 5 mV and the voltage frequencies ranged from 1–10^5 Hz. Supporting electrolyte solution was PBS solution (0.30 M; pH 7.0). The EIS measurements were carried out under open-circuit conditions. The reported result for every electrode in this paper was the mean value of three parallel measurements.

m-Aminobenzenesulfonic acid (purity >98.0%) was purchased from Fluka (USA). Titanium dioxide (TiO_2) nanoparticles were provided by College of Material Science and Engineering, Qingdao University of Science and Technology and used without further purification. Sodium dodecylsulfate (SDS) was purchased from Shanghai Reagent Company (Shanghai, China) and used as received. Tris(hydroxymethyl)amminomethane (Tris) was purchased from Sigma (St. Louis, MO, USA). PCl_5 was purchased from Sinopharm Chemical Reagent Co. (Shanghai, China). All the chemicals were of analytical grade and solutions were prepared with Aquapro ultrapure H_2O (Ever Young Enterprises Development. Co., Chongqing, China).

The 18-base synthetic oligonucleotides probe (pDNA), its cDNA (target DNA, namely a 18-base fragment of CaMV35S gene sequences), double-base mismatched DNA and ncDNA were synthesized by Beijing SBS Gene Technology Co. Ltd (Beijing China). Their base sequences were as follows:

pDNA : 5′-NH_2-TCT TTG GGA CCA CTG TCG-3′

cDNA : 5′-CGA CAG TGG TCC CAA AGA-3′

double-base mismatched DNA : 5′-CGA *A*AG TGG TCC *G*AA AGA-3′

ncDNA : 5′-GCA TCG AGC GAG CAC GTA-3′

All oligonucleotide stock solutions of 18-base oligomers (1.0×10^{-5} M) were prepared by using Tris–HCl solution (pH 7.0), which were stored at 4 °C. More diluted solutions were obtained by diluting an aliquot of the stock solution with ultrapure H_2O prior to use. The hybridization solution was diluted with 2×SSC (pH 7.0).

Electrochemical fabrication of PABSA/TiO_2 nanosheets: The fabrication of CPE was carried out by using a method of Jiang.[46] TiO_2 colloid (0.01 M; 25 μL) was dripped onto the fresh surface of CPE and naturally dried in the air to form TiO_2/CPE. Then it was immersed in a solution of ABSA (0.04 M; containing 0.50 M H_2SO_4) for electropolymerization by PPM. The electropolymerization optimal parameters were listed as follows: upper limit potential E_a, 2.2 V, lower limit potential E_c, −0.5 V, and anodic pulse duration t_a, 0.7 s, cathodic pulse duration t_c, 0.3 s, and total

pulse time t_{exp}, 500 s. On completion of the electropolymerization, a black nanosheets layer was formed on the electrode surface.

Immobilization and hybridization of pDNA on the nanosheet-modified electrode: The immobilization of pDNA on the electrode surface could be accomplished by electrostatic adsorption, covalent binding, and so on. Covalent binding is a better strategy to immobilize biomolecules for better probe orientation while increasing the probe density through increasing the linker density in the film.[47] Here, the pDNA was covalently attached on the PABSA/TiO_2/CPE through the free amines of DNA sequence by using the acyl chloride cross-linking reaction.[30] The sulfonic acid groups of PABSA/TiO_2/CPE were activated by immersing the modified electrode in an acetone solution containing PCl_5 (40 mM) for 0.5 h. The linker/PABSA/TiO_2/CPE was rinsed with Tris–HCl solution (pH 7.0) to wash off the excess PCl_5. Tris–HCl buffer solution (10.0 μL; pH 7.0) containing pDNA (1.0 μM) was then pipetted onto the modified electrode and air-dried to dryness. The electrode surface was washed with ultrapure H_2O to remove the unbound oligonucleotides. Further, the hybridization reaction was carried out by transferring hybridization solution (10 μL; 2× SSC buffer; pH 7.0) containing cDNA onto the probe-modified electrode, followed by thoroughly washing the electrode with 0.2% SDS solution to remove the unhybridized oligonucleotides. The same procedure as mentioned above was applied to the probe-modified electrode for hybridization with double-base mismatched and non-complementary sequences.

Acknowledgements

This work was supported by the National Natural Science Foundation of China (No. 20635020, 20805025, 20975057), the Doctoral Foundation of the Ministry of Education of China (No. 20060426001), the Foundation of Qingdao City (No. 09-1-3-25-jch) and the Doctoral Fund of QUST (0022278).

[1] Y. C. Zhang, H. H. Kim, A. Heller, *Anal. Chem.* **2003**, *75*, 3267–3269.
[2] S. D. Keighley, P. Li, P. Estrela, P. Migliorato, *Biosens. Bioelectron.* **2008**, *23*, 1291–1297.
[3] C. P. Chen, A. Ganguly, C. H. Wang, C. W. Hsu, S. Chattopadhyay, Y. K. Hsu, Y. C. Chang, K. H. Chen, L. C. Chen, *Anal. Chem.* **2009**, *81*, 36–42.
[4] F. R. R. Teles, L. P. Fonseca, *Talanta* **2008**, *77*, 606–623.
[5] M. J. Heller, *Annu. Rev. Biomed. Eng.* **2002**, *4*, 129–153.
[6] K. J. Odenthal, J. J. Gooding, *Analyst* **2007**, *132*, 603–610.
[7] D. Kato, N. Sekioka, A. Ueda, R. Kurita, S. Hirono, K. Suzuki, O. Niwa, *Angew. Chem.* **2008**, *120*, 6783–6786; *Angew. Chem. Int. Ed.* **2008**, *47*, 6681–6684.
[8] B. Piro, J. Haccoun, M. C. Pham, L. D. Tran, A. Rubin, H. Perrot, C. Gabrielli, *J. Electroanal. Chem.* **2005**, *577*, 155–165.
[9] H. Peng, C. Soeller, M. B. Cannell, G. A. Bowmaker, R. P. Cooney, J. Travas-Sejdic, *Biosens. Bioelectron.* **2006**, *21*, 1727–1736.
[10] C. Gautier, C. Cougnon, J. F. Pilard, N. Casse, B. Chenais, M. Laulier, *Biosens. Bioelectron.* **2007**, *22*, 2025–2031.
[11] S. D. Keighley, P. Estrela, P. Li, P. Migliorato, *Biosens. Bioelectron.* **2008**, *24*, 906–911.
[12] S. J. Park, T. A. Talon, C. A. Mirkin, *Science* **2002**, *295*, 1503–1506.
[13] X. Y. Yang, Y. H. Lu, Y. F. Ma, Z. F. Liu, F. Du, Y. S. Chen, *Biotechnol. Lett.* **2007**, *29*, 1775–1779.
[14] N. Prabhakar, H. Singh, B. D. Malhotra, *Electrochem. Commun.* **2008**, *10*, 821–826.
[15] T. Yang, N. Zhou, Y. C. Zhong, W. Zhang, K. Jiao, G. C. Li, *Biosens. Bioelectron.* **2009**, *24*, 2165–2170.
[16] H. X. Chang, Y. Yuan, N. L. Shi, Y. F. Guan, *Anal. Chem.* **2007**, *79*, 5111–5115.
[17] J. Tarver, J. E. Yoo, T. J. Dennes, J. Schwartz, Y. L. Loo, *Chem. Mater.* **2009**, *21*, 280–286.
[18] J. Yue, A. J. Epstein, *J. Am. Chem. Soc.* **1990**, *112*, 2800–2801.
[19] S. A. Kumar, S. M. Chen, *J. Mol. Catal. A* **2007**, *278*, 244–250.
[20] F. X. Gao, R. Yuan, Y. Q. Chai, S. H. Chen, S. R. Cao, M. Y. Tang, *J. Biochem. Biophys. Methods* **2007**, *70*, 407–413.
[21] L. Zhang, X. Jiang, L. Niu, S. J. Dong, *Biosens. Bioelectron.* **2006**, *21*, 1107–1115.
[22] G. Y. Jin, Y. Z. Zhang, W. G. Cheng, *Sensor. Actuat. B* **2005**, *107*, 528–534.
[23] S. A. Kumar, S. M. Chen, *Sensor. Actuat. B* **2007**, *123*, 964–977.
[24] P. H. Lo, S. A. Kumar, S. M. Chen, *Colloids Surf. B* **2008**, *66*, 266–273.
[25] W. Lu, Y. Jin, G. Wang, D. Chen, J. H. Li, *Biosens. Bioelectron.* **2008**, *23*, 1534–1539.
[26] Y. Otsuka, Y. Okamoto, H. Y. Akiyama, K. Umekita, Y. Tachibana, S. Kuwabata, *J. Phys. Chem. C* **2008**, *112*, 4767–4775.
[27] R. Khan, M. Dhayal, *Electrochem. Commun.* **2008**, *10*, 263–267.
[28] J. M. Ashcroft, W. W. Gu, T. R. Zhang, S. M. Hughes, K. B. Hartman, C. Hofmann, A. G. Kanaras, D. A. Kilcoyne, M. L. Gros, Y. D. Yin, A. P. Alivisatos, C. A. Larabell, *Chem. Commun. (Cambridge)* **2008**, 2471–2473.
[29] L. J. Zhang, M. X. Wan, *J. Phys. Chem. B* **2003**, *107*, 6748–6753.
[30] J. H. Chen, J. Zhang, K. Wang, X. H. Lin, L. Y. Huang, G. N. Chen, *Anal. Chem.* **2008**, *80*, 8028–8034.
[31] W. Zhang, T. Yang, C. X. Yin, G. C. Li, K. Jiao, *Electrochem. Commun.* **2009**, *11*, 783–786.
[32] A. Kitani, M. Kaya, S. I. Tsujioka, K. Sasaki, *J. Polym. Sci. Polym. Chem. Ed.* **1988**, *26*, 1531–1539.
[33] X. H. Gao, W. Z. Wei, L. Yang, M. L. Guo, *Electroanalysis* **2006**, *18*, 485–492.
[34] W. Chanmanee, A. Watcharenwong, C. R. Chenthamarakshan, P. Kajitvichyanukul, N. R. de Tacconi, K. Rajeshwar, *J. Am. Chem. Soc.* **2008**, *130*, 965–974.
[35] H. H. Zhou, J. B. Wen, X. H. Ning, C. P. Fu, J. H. Chen, Y. F. Kuang, *Synth. Met.* **2007**, *157*, 98–103.
[36] J. Y. Liu, S. J. Tian, W. Knoll, *Langmuir* **2005**, *21*, 5596–5599.
[37] X. Q. Lin, G. F. Kang, L. P. Lu, *Bioelectrochemistry* **2007**, *70*, 235–244.
[38] M. C. Pham, B. Piro, L. D. Tran, *Anal. Chem.* **2003**, *75*, 6748–6752.
[39] J. J. Gooding, A. Chou, F. J. Mearns, E. Wong, K. L. Jericho, *Chem. Commun. (Cambridge)* **2003**, 1938–1939.
[40] E. Katz, I. Willner, *Electroanalysis* **2003**, *15*, 913–947.
[41] W. Zhang, T. Yang, X. M. Zhuang, Z. Y. Guo, K. Jiao, *Biosens. Bioelectron.* **2009**, *24*, 2417–2422.
[42] T. Y. Lee, Y. B. Shim, *Anal. Chem.* **2001**, *73*, 5629–5632.
[43] H. Cai, Y. Xu, P. G. He, Y. Z. Fang, *Electroanalysis* **2003**, *15*, 1864–1870.
[44] W. M. Zheng, L. He, *J. Am. Chem. Soc.* **2009**, *131*, 3432–3433.
[45] W. S. Yang, J. E. Butler, J. N. Russell, Jr., R. J. Hamers, *Langmuir* **2004**, *20*, 6778–6787.
[46] C. Jiang, T. Yang, K. Jiao, H. W. Gao, *Electrochim. Acta* **2008**, *53*, 2917–2924.
[47] W. Chen, Z. S. Lu, C. M. Li, *Anal. Chem.* **2008**, *80*, 8485–8492.

Received: July 7, 2009
Published online: December 17, 2009

